



Universal Filtered Multicarrier Receiver Complexity Reduction to Orthogonal Frequency Division Multiplexing Receiver

R. Manda*, R. Gowri

Department of Electrical and Electronics, School of Engineering, UPES, Dehradun, India

PAPER INFO

Paper history:

Received 12 November 2021

Received in revised form 08 January 2022

Accepted 09 January 2022

Keywords:

Fifth Generation

Bit Error Rate

Complexity Reduction Ratio

Fast Fourier Transform

Finite Impulse Response

Signal to Noise Ratio

Universal Filtered Multicarrier

ABSTRACT

The Universal Filtered Multicarrier (UFMC) waveform technology is one of the promising waveforms for 5G and beyond 5G networks. Owing 2N-point Fast Fourier Transform (FFT) processor at the UFMC receiver, the computational and implementation complexity is two times more than the conventional Orthogonal Frequency Division Multiplexing (OFDM) receiver system. In this paper, we proposed a simplified UFMC receiver structure to reduce computational complexity as well as hardware requirements. The received UFMC symbol simplified exactly to its equivalent after performing 2N-point FFT and decimation operations. In which, the mathematical model of the frequency-domain UFMC signal is rederived after processing through 2N-point FFT and decimator, and the simplified signal is generated with an N-point FFT. Accordingly, the 2N-point FFT processor and decimator are replaced with a single N-point FFT processor. This approach reduces the 50% computational complexity at the FFT processor level hence the hardware and processing time. The computational complexity of the proposed receiver model is approximately equivalent to the OFDM receiver. Additionally, analyzed the mathematical model for the simplified UFMC receiver and the comparative performance of the UFMC system with the conventional model.

doi: 10.5829/ije.2022.35.04a.12

NOMENCLATURE

$f_p[l]$	The impulse response of p^{th} sub-band filter	$Y_{2N}[k]$	2N-point DFT of $y_{i,zp}[n]$
$f[l]$	Desired/ideal filter impulse response	W_N	The twiddle factor of N-point DFT $W_N = e^{-\frac{j2\pi}{N}}$
$h[n]$	The impulse response of the wireless channel	L_f	Length of the sub-band filter
$S_{ip}[k]$	p^{th} sub-band input constellation mapped data sequence of i^{th} UFMC symbol	L_h	Length of the wireless channel
$s_{ip}[n]$	The output of N-point IFFT block of p^{th} sub-band	N	Size of the IFFT block
$x_i[n]$	The final i^{th} UFMC symbol	N_b	Number of sub-bands
$x_{ip}[n]$	p^{th} sub-band filter output of i^{th} UFMC symbol	Q	Number of data subcarriers per sub-band
$y_i[n]$	The received i^{th} UFMC symbol	V_{sc}	Half of the virtual sub-carriers
$y_{i,zp}[n]$	The received i^{th} UFMC symbol after zeros padded to $y_i[n]$		

1. INTRODUCTION

The ongoing fifth-generation (5G) systems continue to reveal the inherent limitations due to the rise of intelligent communication environments, and some 5G application use cases like massive machine-type communications

(mMTC), and ultra-reliable low latency communications (URLLC) [1]. These limitations are motivation to define the technical requirements and targets of the next-generation (6G) cellular networks that can transfer beyond personalized communication toward the full realization of the Internet of Things (IoT) standard, that

*Corresponding Author Institutional Email: rmanda@ddn.upes.ac.in
(R. Manda)

connects everything, not just people, but also sensors, vehicles, wearables, computing resources, and even robotic agents [2–4]. Therefore, 5G and beyond 5G network use cases complicate the required specifications in many aspects such as data rate, delay or latency, reliability, energy consumption, multicast connectivity, and the type of protocols that provides diverse ways to exchange information between the devices [5]. These systems are impacted by the modulation format used at the physical layer [6–8].

In the last few years, several physical layer waveforms have been proposed like Filter bank multicarrier (FBMC) [9], generalized frequency division multiplexing (GFDM) [10], filtered orthogonal frequency division multiplexing (F-OFDM) [11], and universal filtered multicarrier (UFMC) [12]. Out of these, the UFMC waveform technique is one of the competitive modulation schemes for future generation wireless systems to provide flexible packet transmission services, low interference due to OBE, and relaxed synchronization [13, 14]. However, the transmitter and receiver complexity of UFMC is higher compared to the conventional (CP-OFDM) due to its filtering operation at the transmitter and 2N-point FFT processor at the receiver. To reduce the system complexity and to improve the energy efficiency, the baseband signal processing time and hardware requirement for the new modulation waveform can be reduced by simplifying the structure of the transceiver architecture in terms of computations. In recent years, some methods have been proposed to reduce the computational complexity of the UFMC transmitter [15–18]. The transmitter complexity was reduced by approximating the frequency domain UFMC signal [15], by introducing the FIR filter structure and the poly-phase filter structure based on the lightweight method into the UFMC transmitter structure [17]. A reduced hardware complexity solution [16] was proposed for the implementation of IFFT and filtering operation by avoiding redundant computations. Recently, a reconfigurable baseband UFMC transmitter architecture was proposed by Kumar et al. [18], which has the flexibility to choose the number of subcarriers per sub-band and the pulse-shaping filter. Wu et al. [19] have proposed an advanced receiver for UFMC, which uses the odd number samples of 2N-point FFT along with even number samples to improve the performance at high computations, and here the computational complexity burden of 2N-point FFT has not been reduced. The FFT pruning approach [20], in which removing the operations related to the zero inputs reduces the computational complexity of the UFMC transmitter and receiver. In this paper, the method mainly focused on the system complexity, baseband signal processing latency, and power consumption at the receiver. The proposed approach simplifies the UFMC receiver model, which uses a single N-point FFT to generate the frequency-

domain baseband signal for data detection like the conventional OFDM. This approach avoids the zero-padding operation and decimation part at the UFMC receiver baseband signal processing. Therefore, UFMC reduces the hardware requirement, computational complexity, and hence latency and power consumption. The FFT pruning approach at the UFMC receiver gives fewer computations compared to the conventional model but requires high-level reprogramming since the non-zero inputs vary over time. However, the proposed model requires a smaller number of computations compared to the conventional and the FFT pruning algorithm [20] which is clearly explained in the result analysis session. One of the minor drawbacks of the proposed model is that the hardware implementation needs to use L_f+L_b-2 number of adders before the N-point FFT, which may cause the rise of connectivity complexity and word length effect when it processes through the FFT processor. Otherwise, the proposed model is superior to the conventional model.

The rest of the paper is organized as follows; section 2 described the conventional UFMC transceiver model, section 3 explained the proposed UFMC receiver model that how it is derived from the traditional UFMC receiver model, and section 4 discusses the computational complexity. Section 5, described the performance analysis in terms of complexity and SNR versus BER, and finally, concluded in section 6.

2. CONVENTIONAL UFMC SYSTEM MODEL

2.1. The UFMC Transmitter Model The UFMC waveform technique is a generalized form of OFDM and FBMC, in which a group of subcarriers is individually filtered with a bandpass filter [12]. The schematic block diagram of the traditional UFMC transceiver model is depicted in Figure 1. Whereat the UFMC transmitter, the entire frequency band (total subcarrier) is divided into several blocks (a group of sub-carriers) called sub-band and filtered individually. The final i^{th} UFMC time-domain symbol is the sum of the outputs of all sub-band filters, which can be expressed as

$$x_i[n] = \sum_{p=0}^{N_b-1} x_{ip}[n] \quad (1)$$

The p^{th} sub-band filter output of i^{th} UFMC symbol

$$x_{ip}[n] = \sum_{l=0}^{L_f-1} f_p[l] s_{ip}[n-l]; \quad n = 0, 1, 2, \dots, N + L_f - 2 \quad (2)$$

where $f_p[l]$; $l = 0, 1, \dots, L_f - 1$ is p^{th} sub-band filter impulse response, which is the frequency-shifted version of prototype filter $f[l]$ to the center of p^{th} sub-band.

$$f_p[l] = f[l] e^{j\frac{2\pi}{N}(v_{sc} + (p-\frac{1}{2})Q + \frac{N}{2})l} \quad (3)$$

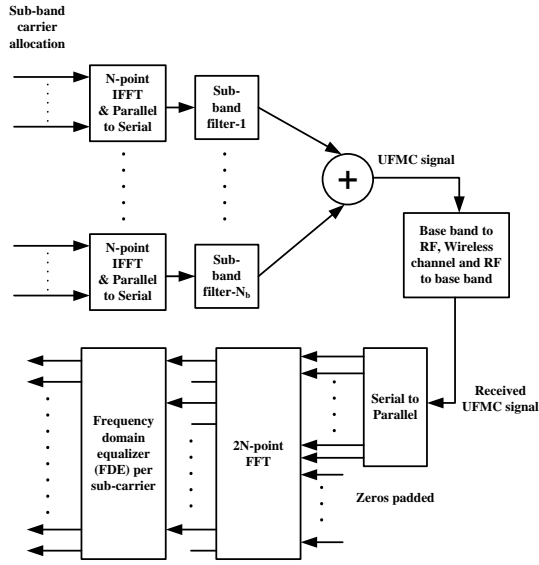


Figure 1. Traditional UFMC transceiver model

The output of the N-point IFFT $s_{ip}[n]$ can be written as

$$s_{ip}[n] = \frac{1}{N} \sum_{k=0}^{N-1} S_{ip}[k] e^{j\frac{2\pi}{N}kn}; n = 0, 1, \dots, N-1 \quad (4)$$

The final UFMC symbol $x_i[n]$ with the length of $N + L_f - 1$ transmitted through the wireless channel, which is

$$y_i[n] = x_i[n] * h[n] + z[n]; n = 0, 1, \dots, N_T - 1 \quad (5)$$

where $z[n]$ is a complex-valued Additive White Gaussian noise (AWGN) with zero mean and variance of σ_z^2 , $N_T = N + L - 2$ and $L = L_f + L_h$.

2.2. The UFMC Receiver Model At the receiver, the zeroes padded to the received symbol to perform the 2N-point FFT to consider the sub-band filter tails. The received signal after zeros padded

$$y_{i,zp}[n] = \begin{cases} y_i[n]; & 0 \leq n \leq N_T - 1 \\ 0; & N_T \leq n \leq 2N - 1 \end{cases} \quad (6)$$

The frequency-domain of the received UFMC signal after processing through the 2N-point FFT is mathematically formulated as

$$Y_{2N}[k] = \sum_{n=0}^{2N-1} y_{i,zp}[n] W_{2N}^{kn}; k = 0, 1, \dots, 2N-1 \quad (7)$$

The receiver only needs to extract the even-numbered samples after the 2N-point FFT transformation to estimate the data symbols because the odd-numbered samples consist of an interference component (proof can see in the appendix). In conventional UFMC receiver, this is implemented with 2N-point FFT and decimator with factor 2 shown in Figure 1, which is twice the size of FFT that is used in conventional OFDM receiver and increases the UFMC receiver complexity compared to the OFDM receiver.

2.3. Data Detection The final UFMC transmitted symbol $x(n)$ having the length $N + L_f - 1$, can be expressed in matrix form as

$$X = \sum_{p=1}^B [F_p]_{(N+L_f-1) \times N} [V_p]_{N \times Q} [S_p]_{Q \times 1} \quad (8)$$

where $[F_p]_{(N+L_f-1) \times N}$ is a Toeplitz matrix of p^{th} sub-band FIR filter impulse response with the first column $[f_p(0), f_p(1), \dots, f_p(L_f - 1), [0]_{1 \times N-1}]^T$ and first row $[f_p(0), [0]_{1 \times N-1}]$, $[V_p]_{N \times Q}$ is the IFFT matrix that relevant to p^{th} sub-band carriers and S_p is the column matrix of the p^{th} sub-band data sequence.

$$X = \mathcal{F}\mathcal{V}\mathcal{S} \quad (9)$$

$$\begin{aligned} \mathcal{F} &= [F_0, F_1, \dots, F_{B-1}] \\ \mathcal{V} &= \text{blockdiag}([V_0, V_1, \dots, V_{B-1}]) \\ \mathcal{S} &= [S_0^T, S_1^T, \dots, S_{B-1}^T]^T \end{aligned}$$

This UFMC symbol is transmitted through the wireless channel, which can be defined as

$$y = HX + z = \mathcal{H}\mathcal{F}\mathcal{V}\mathcal{S} + z \quad (10)$$

where \mathcal{H} is the Toeplitz matrix of the channel coefficients $h(n)$ with the first column $[h(0), h(1), \dots, h(L_h - 1), [0]_{1 \times N+L_f-2}]^T$ and first row $[h(0), [0]_{1 \times N+L_f-2}]$ and z is the zero mean Additive White Gaussian Noise (AWGN) vector having length $N + L - 2$. After performing the 2N-point FFT, the even-numbered frequency domain samples are

$$Y_e = \mathcal{P}_e \mathcal{W} \mathcal{H} \mathcal{F} \mathcal{V} \mathcal{S} + \mathcal{P}_e^T \mathcal{W} z \quad (11)$$

where the matrix $[\mathcal{P}_e]_{N \times 2N}$ with elements

$$\mathcal{P}_e(m, k) = \begin{cases} 1; & \text{for } k = 2m \\ 0; & \text{for } k \neq 2m \end{cases} \quad (12)$$

where $m = 0, 1, \dots, N-1$ and $k = 0, 1, \dots, 2N-1$. Where $[\mathcal{W}]_{2N \times (N+L-2)}$ are the 2N-point FFT twiddle factor matrix and its elements are $\mathcal{W}(k, r) = W_{2N}^{kr}$; where $k = 0, 1, \dots, 2N-1$; and $r = 0, 1, \dots, N+L-3$. These even-numbered samples are used for data detection. By Least squares algorithm, the estimated data sequence is defined as

$$\hat{S} = (A^H A)^{-1} A^H Y_e; A = \mathcal{P}_e^T \mathcal{W} \mathcal{H} \mathcal{F} \mathcal{V} \quad (13)$$

3. THE PROPOSED UFMC RECEIVER MODEL

The even-numbered samples/sub-carriers of 2N-point FFT are defined as

$$Y_e[k] = Y_{2N}[2k] = \sum_{n=0}^{2N-1} y_{i,zp}[n] W_{2N}^{2kn}; k = 0, 1, \dots, N-1 \quad (14)$$

We know that

$$W_{2N}^{2kn} = e^{-\frac{j2\pi}{2N}2kn} = e^{-\frac{j2\pi}{N}kn} = W_N^{kn} \quad (15)$$

We rewrite Equation (8) as

$$Y_e[k] = \sum_{n=0}^{2N-1} y_{i,zp}[n] W_N^{kn} = \sum_{n=0}^{N-1} y_{i,zp}[n] W_N^{kn} + \sum_{n=N}^{2N-1} y_{i,zp}[n] W_N^{kn} \quad (16)$$

Let assume that $m = n - N$, then, Equation (16) can be rewritten as

$$Y_e[k] = \sum_{n=0}^{N-1} y_{i,zp}[n] W_N^{kn} + \sum_{m=0}^{N-1} y_{i,zp}[m+N] W_N^{k(m+N)} \quad (17)$$

where $W_N^{kN} = e^{-\frac{j2\pi}{N}kN} = e^{-j2\pi k} = 1$

$$Y_e[k] = \sum_{n=0}^{N-1} y_i[n] W_N^{kn} + \sum_{m=0}^{L-3} y_i[m+N] W_N^{km} \quad (18)$$

Finally, Equation (18) can be written as

$$Y_e[k] = \sum_{n=0}^{N-1} y'[n] W_N^{kn} \quad (19)$$

where

$$y'[n] = \begin{cases} y_i[n] + y_i[n+N]; & 0 \leq n \leq L-3 \\ y_i[n]; & L-2 \leq n \leq N-1 \end{cases} \quad (20)$$

Now, according to Equation (20) the even-numbered subcarriers can be generated with a single N-point FFT having $y'[n]$ as input, which is shown in Figure 2. Here, both the 2N-point DFT and decimator operations can be implemented with the single N-point DFT. The computational complexity can be reduced twice compared to the conventional UFMC receiver.

4. COMPLEXITY ANALYSIS OF THE PROPOSED MODEL

The major computational complexity in the UFMC receiver system includes the 2N-point FFT processor, the channel estimation, and equalization algorithms. The UFMC baseband signal model at the receiver is like the OFDM signal except for the filter equalization, so, the same algorithms can be applied in the UFMC system for channel estimation and equalization. Therefore, the

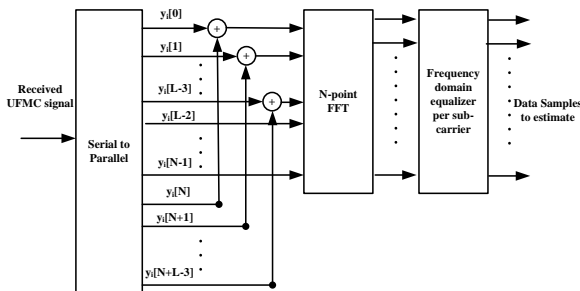


Figure 2. Block diagram of the proposed UFMC receiver model

UFMC receiver complexity is two times higher compared to the OFDM receiver. Furthermore, the additional memory or control overhead is one of the main disadvantages of the implementation.

The N-point DFT is efficiently computed by the FFT algorithm [21], which requires the total number of arithmetic operations (real multiplications and additions) using radix-2 FFT algorithm is $5N \log_2 N$. The split-radix FFT algorithm [22] has a lower number of arithmetic operations compared to the radix-2 FFT algorithm, which requires the total number of arithmetic operations to be $4N \log_2 N - 6N + 8$. With the FFT pruning algorithm, the number of real operations (additions and multiplications) required to process the UFMC baseband received signal [20] is $5N \log_2 N - 2N + 4(L - 2)$. Table 1 describes the computational complexity comparison between the conventional, FFT pruning approach and the proposed receiver model. Which states that the proposed UFMC receiver model has a smaller number of arithmetic operations, it is simple and effective compared to conventional CP-OFDM and UFMC receivers. The complexity efficiency of the system can be measured by complexity reduction ratio (CRR), which is defined as the ratio of the total number of computations required for the conventional model (CM_{ufmc}^{conv}) to the total number of computations required for the conventional model (CM_{ufmc}^{prop}).

$$CRR = \frac{CM_{ufmc}^{conv}}{CM_{ufmc}^{prop}} \approx 2 \left(1 + \frac{1}{\log_2 N} \right) \quad (21)$$

From Equation (21), the proposed model reduces the computational complexity more than two times as compared to the conventional UFMC receiver model. Also, in the proposed model, there are no zeros padding operations to process through 2N-point FFT. Therefore, the number of read/ write memory locations was reduced by two times approximately. However, the required storage space for read/ write operations is the same as the conventional OFDM receiver model. In the proposed

TABLE 1. Computational complexity comparison

Receiver model type	Number arithmetic operations (CM)	Required hardware blocks for the baseband signal processing at the receiver
CP-OFDM receiver	$4N \log_2 N - 6N + 8$	CP remover, N-point FFT, FDE
Conventional UFMC receiver	$8N \log_2 N - 4N + 8$	Zeros padder, 2N-point FFT, Decimator, FDE
UFMC receiver with FFT pruning	$5N \log_2 N - 2N + 4(L - 2)$	Zeros padder, 2N-point FFT, FDE
Proposed UFMC receiver	$4N \log_2 N - 6N + 8 + 2(L - 2)$	N-point FFT, FDE

model, the adder blocks are used before N-point FFT which may increase the connectivity complexity compared to the traditional model.

The power carried by odd-numbered frequency samples of 2N-point FFT is not utilized in the conventional UFMC receiver, hence the power efficiency is 50%. But in the proposed model, there is no 2N-point FFT and which uses all the samples processed by FFT. Therefore, the power efficiency can be improved to 100%. Finally, we can say that the proposed UFMC receiver model is more suitable for ultra-low latency and low energy consumption IoT uses cases as well as for next-generation cellular networks.

5. SIMULATION RESULTS

The computational complexity of the receiver depends only on the size of the FFT. In this session, some computer simulation results are presented. The numerical analysis of computational complexity and its comparison is shown in Figure 3 for different bandwidth (BW) configurations mentioned in Table 2 under the NR-TDL vehicular-A channel model with a length of 24. These comparisons conclude that the proposed receiver model has a lesser number of arithmetic operations (i.e., two times lesser) at the baseband FFT signal processing level compared conventional model and almost achieved the same computational complexity of the CP-OFDM receiver. Furthermore, the complexity ratio (CR) of the UFMC receiver to the OFDM receiver $\left(\frac{CM_{ufmc}}{CM_{ofdm}}\right)$ for different methods are shown in Figure 4. Consider the bandwidth of 20 MHz and $N = 1024$ for numerical comparison between the proposed and conventional models, in this case, the CR values are 2.1904, 1.3881, and 1.0036 for the conventional, conventional with FFT pruning algorithm and the proposed UFMC receiver model respectively. From these numerical analyses, the proposed model has less complexity ratio and is more

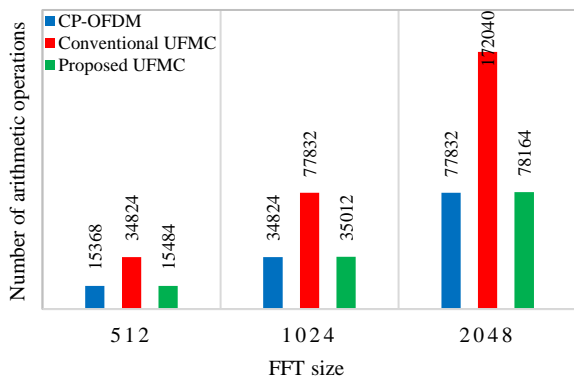


Figure 3. Comparison of computational complexity (with split-radix FFT algorithm)

TABLE 2. Bandwidth configuration for NR frequency band range (FR)-1 for SCS = 15 kHz [23]

Bandwidth/specifications	5 MHz	10 MHz	20 MHz
Number of subcarriers	333	666	1333
Data subcarrier	300	624	1272
FFT/IFFT size	512	1024	2048
CP length = $L_f - 1$	36	72	144

efficient in terms of computational complexity. Also, the FFT's per energy [24] can be improved, which is defined as

$$FFT's/Energy = \frac{Technology}{Power \times Execution\ time \times 10^{-6}} \quad (22)$$

where Technology is the CMOS process in micrometers, the power consumption is proportional to supply voltage, clock frequency, and load capacitance. The execution time depends on the number of operations/computations required to complete a particular task. From Equation (22), the FFT's per energy is inversely proportional to the execution time, which means for the proposed model the FFT processor requires lesser execution time compared to the conventional one. Finally, we can say that the proposed UFMC receiver model is more suitable for ultra-low latency and low energy consumption uses cases of the next-generation cellular networks.

The proposed model is a simplified model of the conventional model. Therefore, it gives almost the same performance in terms of SNR versus BER at lower computational cost, which is shown in Figure 5 for the simulation parameters mentioned in Table 3.

In practical cases due to the additional adders on the receiver side, the proposed model may increase the connectivity complexity and occurs small losses; hence small performance degradation (shown in Figure 5).

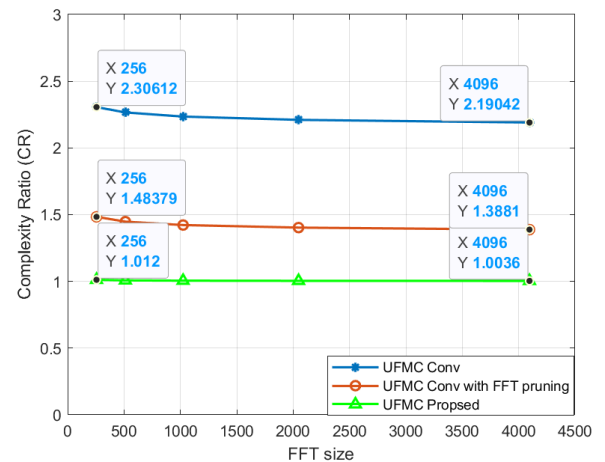


Figure 4. Complexity ratio (CR) of the UFMC receiver to the OFDM receiver

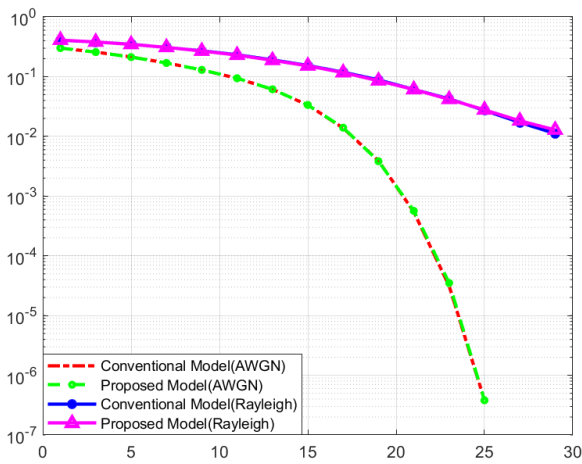


Figure 5. SNR versus BER for UPMC transceiver system

TABLE 3. Simulation parameters

Parameter name	Value
Channel bandwidth	10 MHz
Modulation type	16-QAM
FFT size	1024
CP length	72
Number of UPMC symbols	7
Sub-band size	12
Stopband attenuation (A_s)	40 dB
Channel type	AWGN/ Rayleigh fading

6. CONCLUSION

The UPMC was one of the candidate waveforms for 5G, but the computational and hardware complexity of the UPMC transceiver system has more than the CP-OFDM system due to filtering operation at the transmitter and $2N$ -point FFT processing at the receiver. In this point of view, here we proposed the simplified UPMC receiver model, in which the exact frequency domain UPMC received symbol after FFT processor and decimator is derived and simplified to implement with a single N -point FFT and that reduced the computational complexity more than two times (i.e., 50%) compared to the traditional receiver model without degrading the system performance. At the receiver, the zero-padding for processing $2N$ -point FFT and decimation part is simply replaced by one N -point FFT, which reduced the number of hardware components at baseband signal processing and the storage requirement for read/write operation to process the data and the number of computations or operations. This model reduced the hardware requirement and hence the power consumption. The real-time hardware implementation of this model is the future scope of this work.

7. REFERENCES

- Saad, W., Bennis, M., and Chen, M. "A Vision of 6G Wireless Systems: Applications, Trends, Technologies, and Open Research Problems." *IEEE Network*, Vol. 34, No. 3, (2020), 134–142. <https://doi.org/10.1109/MNET.001.1900287>
- Yang, P., Xiao, Y., Xiao, M., and Li, S. "6G Wireless Communications: Vision and Potential Techniques." *IEEE Network*, Vol. 33, No. 4, (2019), 70–75. <https://doi.org/10.1109/MNET.2019.1800418>
- Zhang, Z., Xiao, Y., Ma, Z., Xiao, M., Ding, Z., Lei, X., Karagiannis, G. K., and Fan, P. "6G Wireless Networks: Vision, Requirements, Architecture, and Key Technologies." *IEEE Vehicular Technology Magazine*, Vol. 14, No. 3, (2019), 28–41. <https://doi.org/10.1109/MVT.2019.2921208>
- Giordani, M., Polese, M., Mezzavilla, M., Rangan, S., and Zorzi, M. "Toward 6G Networks: Use Cases and Technologies." *IEEE Communications Magazine*, Vol. 58, No. 3, (2020), 55–61. <https://doi.org/10.1109/MCOM.001.1900411>
- Raza, R., and Al-Ani, M. "Routing Protocols for IOT Applications based on Distributed Learning." *International Journal of Engineering, Transaction A: Basics*, Vol. 34, No. 4, (2021), 825–831. <https://doi.org/10.5829/ije.2021.34.04a.08>
- Banelli, P., Buzzi, S., Colavolpe, G., Modenini, A., Rusek, F., and Ugolini, A. "Modulation Formats and Waveforms for 5G Networks: Who Will Be the Heir of OFDM?: An overview of alternative modulation schemes for improved spectral efficiency." *IEEE Signal Processing Magazine*, Vol. 31, No. 6, (2014), 80–93. <https://doi.org/10.1109/MSP.2014.2337391>
- Schulz, P., Matthe, M., Klessig, H., Simsek, M., Fettweis, G., Ansari, J., Ashraf, S. A., Almeroth, B., Voigt, J., Riedel, I., ... Windisch, M. "Latency Critical IoT Applications in 5G: Perspective on the Design of Radio Interface and Network Architecture." *IEEE Communications Magazine*, Vol. 55, No. 2, (2017), 70–78. <https://doi.org/10.1109/MCOM.2017.1600435CM>
- Mukherjee, A. "Energy Efficiency and Delay in 5G Ultra-Reliable Low-Latency Communications System Architectures." *IEEE Network*, Vol. 32, No. 2, (2018), 55–61. <https://doi.org/10.1109/MNET.2018.1700260>
- Farhang-Boroujeny, B. "OFDM Versus Filter Bank Multicarrier." *IEEE Signal Processing Magazine*, Vol. 28, No. 3, (2011), 92–112. <https://doi.org/10.1109/MSP.2011.940267>
- Michailow, N., Matthe, M., Gaspar, I. S., Caldevilla, A. N., Mendes, L. L., Festag, A., and Fettweis, G. "Generalized Frequency Division Multiplexing for 5th Generation Cellular Networks." *IEEE Transactions on Communications*, Vol. 62, No. 9, (2014), 3045–3061. <https://doi.org/10.1109/TCOMM.2014.2345566>
- Zhang, L., Ijaz, A., Xiao, P., Mulu, M. M., and Tafazolli, R. "Filtered OFDM Systems, Algorithms, and Performance Analysis for 5G and Beyond." *IEEE Transactions on Communications*, Vol. 66, No. 3, (2018), 1205–1218. <https://doi.org/10.1109/TCOMM.2017.2771242>
- Vakilian, V., Wild, T., Schaich, F., ten Brink, S., and Frigon, J.-F. "Universal-filtered multi-carrier technique for wireless systems beyond LTE." In 2013 IEEE Globecom Workshops (GC Wkshps) (pp. 223–228). IEEE. <https://doi.org/10.1109/GLOCOMW.2013.6824990>
- Schaich, F., and Wild, T. "Waveform contenders for 5G - OFDM vs. FBMC vs. UPMC." In 2014 6th International Symposium on Communications, Control and Signal Processing (ISCCSP) (pp. 457–460). IEEE. <https://doi.org/10.1109/ISCCSP.2014.6877912>
- Schaich, F., Wild, T., and Chen, Y. "Waveform Contenders for 5G - Suitability for Short Packet and Low Latency

- Transmissions.” In 2014 IEEE 79th Vehicular Technology Conference (VTC Spring) (pp. 1–5). IEEE. <https://doi.org/10.1109/VTCSpring.2014.7023145>
15. Wild, T., and Schaich, F. “A Reduced Complexity Transmitter for UF-OFDM.” In 2015 IEEE 81st Vehicular Technology Conference (VTC Spring) (pp. 1–6). IEEE. <https://doi.org/10.1109/VTCSpring.2015.7145643>
 16. Jafri, A. R., Majid, J., Shami, M. A., Imran, M. A., and Najam-Ul-Islam, M. “Hardware Complexity Reduction in Universal Filtered Multicarrier Transmitter Implementation.” *IEEE Access*, Vol. 5, (2017), 13401–13408. <https://doi.org/10.1109/ACCESS.2017.2728605>
 17. Guo, Z., Liu, Q., Zhang, W., and Wang, S. “Low Complexity Implementation of Universal Filtered Multi-Carrier Transmitter.” *IEEE Access*, Vol. 8, (2020), 24799–24807. <https://doi.org/10.1109/ACCESS.2020.2970727>
 18. Kumar, V., Mukherjee, M., and Lloret, J. “Reconfigurable Architecture of UFMC Transmitter for 5G and Its FPGA Prototype.” *IEEE Systems Journal*, Vol. 14, No. 1, (2020), 28–38. <https://doi.org/10.1109/JSYST.2019.2923549>
 19. Wu, M., Dang, J., Zhang, Z., and Wu, L. “An Advanced Receiver for Universal Filtered Multicarrier.” *IEEE Transactions on Vehicular Technology*, Vol. 67, No. 8, (2018), 7779–7783. <https://doi.org/10.1109/TVT.2018.2831245>
 20. Saad, M., Al-Ghouwayel, A., and Hijazi, H. “UFMC Transceiver Complexity Reduction.” In 2018 25th International Conference on Telecommunications (ICT) (pp. 295–301). IEEE. <https://doi.org/10.1109/ICT.2018.8464863>
 21. Cooley, J. W., and Tukey, J. W. “An Algorithm for the Machine Calculation of Complex Fourier Series.” *Mathematics of Computation*, Vol. 19, No. 90, (1965), 297. <https://doi.org/10.2307/2003354>
 22. Duhamel, P., and Hollmann, H. “ ‘Split radix’ FFT algorithm.” *Electronics Letters*, Vol. 20, No. 1, (1984), 14. <https://doi.org/10.1049/el:19840012>
 23. 3GPP TS 38.101-1 v15.1.0, ‘NR: User Equipment (UE) radio transmission and reception part1., 2011.
 24. Yang, C.-H., Yu, T.-H., and Markovic, D. “Power and Area Minimization of Reconfigurable FFT Processors: A 3GPP-LTE Example.” *IEEE Journal of Solid-State Circuits*, Vol. 47, No. 3, (2012), 757–768. <https://doi.org/10.1109/JSSC.2011.2176163>

APPENDIX

The frequency-domain received UFMC signal after processing through the 2N-point FFT

$$Y_{2N}(k) = \sum_{n=0}^{2N-1} y_{zp}(n) e^{-\frac{j2\pi}{2N}kn} \quad (23)$$

To detect the data from this received signal like in the OFDM system, we require to collect N- samples from 2N- samples and these samples do not contain any interference components. For this purpose, the 2N-samples are divided into even and add number samples.

For even-numbered samples, $k = 0, 2, 2N - 2$ and $k = 2k'$; $k' = 0, 1, \dots, N - 1$ therefore, the even-numbered subcarriers of 2N-point FFT are

$$Y_e(k') = Y_{2N}(2k') = \sum_{n=0}^{2N-1} y_{zp}(n) e^{-\frac{j2\pi}{N}k'n} \quad (24)$$

Similarly, the odd-numbered subcarriers are

$$Y_o(k') = Y_{2N}(2k' + 1) = \sum_{n=0}^{2N-1} y_{zp}(n) e^{-\frac{j2\pi}{2N}(2k'+1)n} = \sum_{n=0}^{2N-1} y_{zp}(n) e^{-\frac{j2\pi}{N}k'n} e^{-\frac{j\pi}{N}n} \quad (25)$$

From Equations (23) and (24), it was observed that the data can be directly retrieved from the even-numbered subcarriers, but it cannot be retrieved from odd-numbered subcarriers due to the presence of interference component. That is why the odd-numbered subcarriers are discarded and even-numbered subcarriers are extracted for data detection at the receiver using a single-tap frequency domain equalizer (FDE).

Persian Abstract

چکیده

فناوری شکل موج چند حامل فیلتر شده جهانی (UFMC) یکی از شکل‌های موج امیدوارکننده برای شبکه‌های 5G و فراتر از آن است. با توجه به پردازشگر تبدیل فوریه سریع (FFT) 2N در گیرنده UFMC، پیچیدگی محاسباتی و پیاده‌سازی دو برابر بیشتر از سیستم گیرنده متعارف تقسیم فرکانس متعامد (OFDM) است. در این مقاله، ما یک ساختار گیرنده UFMC ساده شده را برای کاهش پیچیدگی محاسباتی و همچنین نیازهای سخت‌افزاری پیشنهاد کردیم. نماد دریافتی UFMC دقیقاً پس از انجام عملیات FFT نقطه 2N و حذف دقیقاً به معادل خود ساده شد که در آن، مدل ریاضی سیگنال UFMC حوزه فرکانس پس از پردازش از طریق FFT نقطه 2N و دسیماتور دوباره استخراج می‌شود و سیگنال ساده شده با یک FFT نقطه N تولید می‌شود. بر این اساس، پردازنده FFT 2N و Decimator با یک پردازنده FFT نقطه N جایگزین می‌شود. این رویکرد پیچیدگی محاسباتی را 50٪ در سطح پردازنده FFT کاهش می‌دهد و در نتیجه زمان سخت‌افزار و پردازش را کاهش می‌دهد. پیچیدگی محاسباتی مدل گیرنده پیشنهادی تقریباً معادل گیرنده OFDM است. علاوه بر این، مدل ریاضی برای گیرنده UFMC ساده شده و عملکرد مقایسه‌ای سیستم UFMC با مدل معمولی مورد تجزیه و تحلیل قرار گرفت.
